European Journal of Immunology Clinical·Basic·Translational

Adaptive immunity

Basic

Research Article

# Enhanced Mott cell formation linked with IgM Fc receptor (FcμR) deficiency

*Pedram Mahmoudi Aliabadi*[*,†1], *Khlowd Al-Qaisi*[*1], *Peter K. Jani*[*2], *Kazuhito Honjo*[3], *Uwe Klemm*[4], *Kyeong-Hee Lee*[5], *Nicole Baumgarth*[6], *Andreas Radbruch*[7], *Fritz Melchers*[2] and *Hiromi Kubagawa*[1]

[1] Humoral Immune Regulation, Deutsches Rheuma-Forschungszentrum (DRFZ), Berlin, Germany
[2] Lymphocyte Development, Deutsches Rheuma-Forschungszentrum (DRFZ), Berlin, Germany
[3] Department of Medicine, School of Medicine, University of Alabama, Birmingham, USA
[4] Experimental Animals, Max Planck Institute for Infectious Biology, Berlin, Germany
[5] Inflammation Research Group, Institute of Clinical Chemistry, Hannover Medical School, Hanover, Germany
[6] Department of Molecular Microbiology and immunology, Johns Hopkins Bloomberg School of Public Health, Baltimore, USA
[7] Department of Cell Biology, Deutsches Rheuma-ForschungszentrumDRFZ), Berlin, Germany

**In previous studies, Mott cells, an unusual form of plasma cells containing Ig-inclusion bodies, were frequently observed in peripheral lymphoid tissues in our IgM Fc receptor (FcμR)-deficient (KO) mouse strain. Because of discrepancies in the reported phenotypes of different *Fcmr* KO mouse strains, we here examined two additional available mutant strains and confirmed that such enhanced Mott-cell formation was a general phenomenon associated with FcμR deficiency. Splenic B cells from *Fcmr* KO mice clearly generated more Mott cells than those from WT mice when stimulated in vitro with LPS alone or a B-1, but not B-2, activation cocktail. Nucleotide sequence analysis of the Ig variable regions of a single IgMλ$^+$ Mott-hybridoma clone developed from splenic B-1 B cells of *Fcmr* KO mice revealed the near (VH) or complete (Vλ) identity with the corresponding germline gene segments and the addition of six or five nucleotides at the VH/DH and DH/JH junctions, respectively. Transduction of an FcμR cDNA into the Mott hybridoma significantly reduced cells containing IgM-inclusion bodies with a concomitant increase in IgM secretion, leading to secreted IgM binding to FcμR expressed on Mott transductants. These findings suggest a regulatory role of FcμR in the formation of Mott cells and IgM-inclusion bodies.**

**Keywords:** B-1 B cells · FcμR · Ig-inclusion body · Mott hybridoma · Russel body

Additional supporting information may be found online in the Supporting Information section at the end of the article.

*Correspondence:* Prof. Hiromi Kubagawa
e-mail: hiromi.kubagawa@drfz.de

[*]Pedram Mahmoudi Aliabadi, Khlowd Al-Qaisi, and Peter K. Jani equally contributed to this study.
[†]A candidate for MD/PhD of Charité-Universitätsmedizin Berlin, corporate member of Freie Universität Berlin and Humboldt-Universität zu Berlin.

## Introduction

Mott cells, also called morular or grape cells, are bizarre plasma cells containing Ig-inclusion bodies termed Russell bodies in the cytoplasm [1, 2]. Ultrastructurally, electron-dense Russell bodies are built up within the cisterna of dilated rough ER and represent a cellular response to the accumulation of abundant non-degradable Igs that fail to exit from the ER [3–7]. Mott cells are rarely detected in normal tissues but are frequently observed in various pathological conditions including autoimmune disorders, B-cell neoplasms, and chronic infections [1, 2, 5, 6, 8–14]. Many different causes or factors have been implicated in the formation of Russell bodies and Mott cells. These include (i) structural alterations of Ig heavy chain (HC), especially truncation of the CH1 domain, preventing its appropriate processing, (ii) impairment of Ig light chains (LCs), which normally prevent Ig HC aggregation as shown in Ig LC-deficient mice, and (iii) inability to degrade or to export Ig, leading to its aggregation [15–18].

The Fc receptor for IgM (FcμR), the newest member of the FcR family, is a type I transmembrane sialoglycoprotein with an $M_r$ of ~60 kDa. Unlike FcRs for switched Ig isotypes (e.g. FcγRs, FcεRs, FcαR, Fcα/μR), FcμR is selectively expressed by lymphocytes: B, T, and NK cells in humans and only B cells in mice, although several articles have reported the FcμR expression by non-B cells in mice [19–23]. It exclusively binds IgM, either J-chain-containing pentameric or J-chain-lacking hexameric IgM, with a high affinity of ~10 nM [19, 24]. FcμR more efficiently binds the Fc portion of IgM when it recognizes a membrane component (like a self-antigen) via its Fab region on the same cell surface (*cis* engagement) than the Fc portion of IgM in solution or fluid (*trans* engagement) [25]. In the mouse thymoma line BW5147 stably expressing human or mouse FcμR, the human receptor binds IgM irrespective of the stages of cell growth (constitutive binding), whereas the mouse receptor binds IgM only before the early log stage of cell growth (transient binding), despite there being no significant changes in the receptor levels during cell culture [19, 26]. By taking advantage of this difference in ligand binding, mutational analysis of human FcμR revealed that at least three sites in the Ig-like domain (Asn 66 in CDR2, Lys 79 to Arg83 in DE loop, and Asn109 in CDR3) are responsible for its constitutive ligand binding [27, 28]. To determine the in vivo function of FcμR, four different laboratories have developed five different *Fcmr*-deficient (KO) mice and at least eight different groups of investigators have examined the resultant phenotypes [see review [29]]. Some clear discrepancies have been noted, particularly in FcμR functions of non-B cell populations, that appear to be due to various factors including differences in the exons of *Fcmr* that were targeted to generate the mutant mice [29]. However, one common feature among these different mutant mice is the impairment of B cell tolerance, as evidenced by the propensity to produce autoantibodies of both IgM and IgG isotypes [22, 23, 29–32].

In previous studies, Mott cells were increased in the spleen and LN tissues of our *Fcmr* KO mice [33]. The aim of the present study was to determine if such enhanced Mott cell formation is a general phenomenon associated with FcμR deficiency or a characteristic unique to our mutant strain.

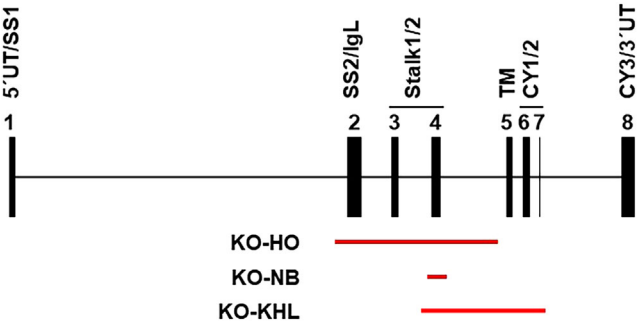


**Figure 1.** Schematic representation of the targeted exons in the *Fcmr* KO mice used in this study. Exons (black closed boxes) of *Fcmr* encoding particular regions of the receptor are denoted as follows: the 5' untranslated (5' UT), the signal peptides (SS1 and SS2), the Ig-like domain (IgL), the uncharacterized extracellular (Stalk 1 and 2), the transmembrane (TM), the cytoplasmic (CY1-3), and the 3' untranslated (3' UT) regions. Red lines indicate the exons targeted in the indicated *Fcmr* KO mouse strain.

## Results

### Enhanced Mott cell formation in three different strains of FcμR-deficient mice

To determine the association of Mott cell formation with FcμR deficiency, we examined the frequency of Mott cells in lymphoid tissues from three available different strains of *Fcmr* KO mice. These mutant mice had been developed by different groups using distinct targeting strategies (see Fig. 1): (i) our strategy (KO-HO) involved the germline deletion of *Fcmr* exon 2 to 4 encoding the Ig-like domain, first and second stalk regions, respectively, and most of intron 4 [22, 23]; (ii) the KO-NB strains involved both generalized and B cell type-specific conditional deletion of exon 4 (second stalk region) [31]; and (iii) the KO-KHL strain involved the B cell type-specific conditional deletion of exon 4 to 7 (second stalk, transmembrane, first and second cytoplasmic regions, respectively) [32].

Mott cells and their inclusion bodies or extracellular spherons were uniquely identified by their strong staining with the periodic acid-Schiff (PAS; Sigma–Aldrich) reagent in the splenic red pulp, because PAS did not stain periodic acid-fixed erythrocytes, and thus, cellular changes in the splenic red pulp were easily detectable (Fig. 2). Mott cells with variable morphologies were scattered in the red pulp and in the medulla and extrafollicular areas of LNs (Figs. 2A and B). They were sometimes clustered (Fig. 2C), suggesting possible local expansion. Mott cells were also often observed in the splenic and nodal serosal fatty tissues (Fig. 2D), consistent with the notion that Mott cells are derived from B-1 B cells present in the peritoneal cavity [11, 34, 35]. Mott cells were also found in the Peyer's patches (Fig. 2E) and the medullary cavity of BM (Fig. 2F); the latter finding raising the possibility that they were either generated in situ or migrated

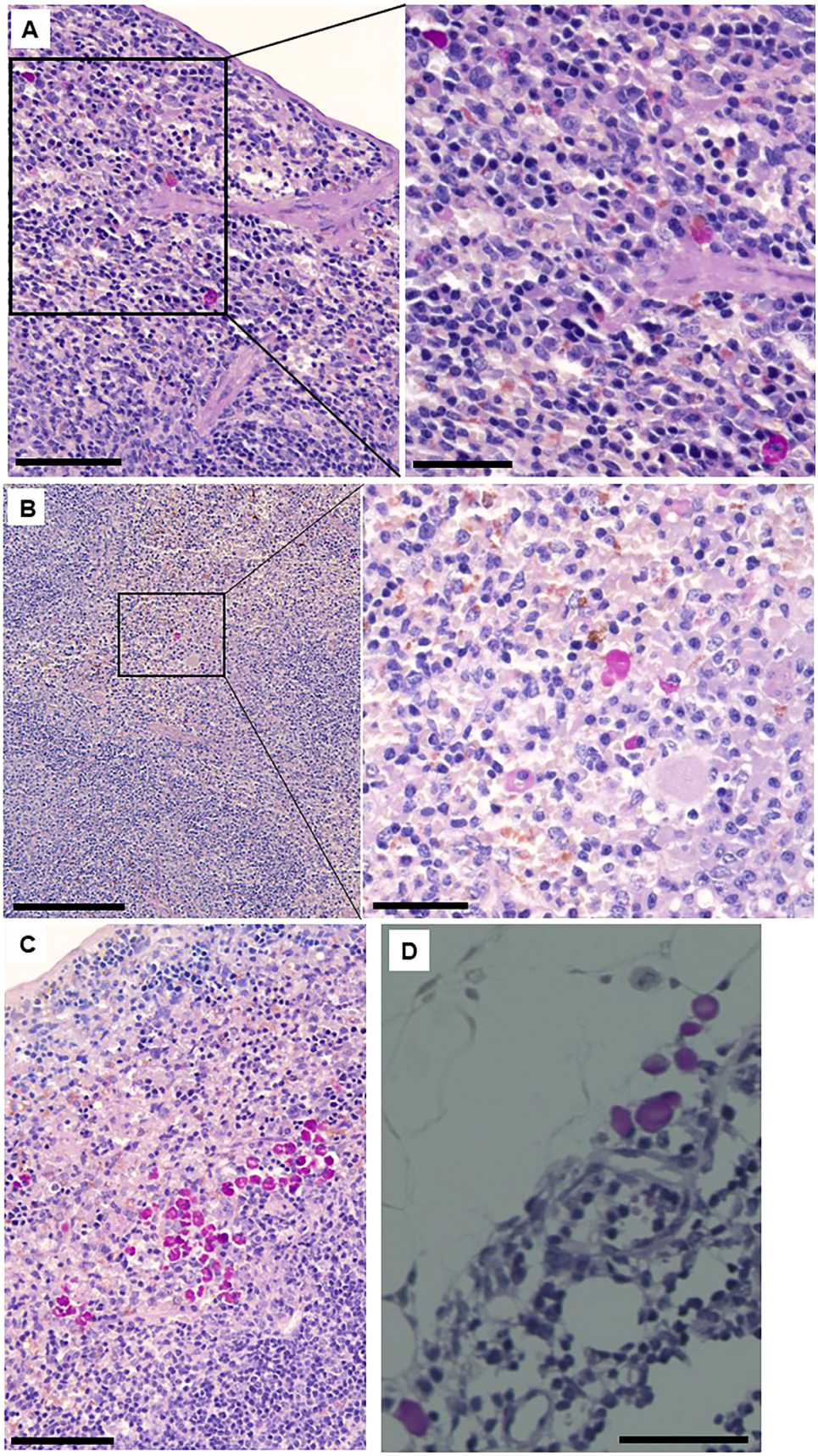


**Figure 2.** Mott cells in tissue sections stained with PAS reagent. (A) Spleen red pulp of KHL-*Cd19*$^{Cre+/-}$ mouse, 200x (left) and 400x (right). (B) Lymph node medulla of HO-*Fcmr* KO mouse, 100×(left) and 400× (right). (C) Spleen red pulp of KHL-*Cd19*$^{Cre+/-}$ mouse, 200×. (D) Splenic serosal fatty tissue of NO-CMV KO mouse, 400×. (E) Peyer patch of HO-*Fcmr* KO mouse, 100× (left) and 400× (right). (F) Bone marrow of HO-*Fcmr* KO mouse, 400×. Scale bars in each magnification indicate 200 μm for 100×, 80 μm for 200×, and 40 μm for 400×.

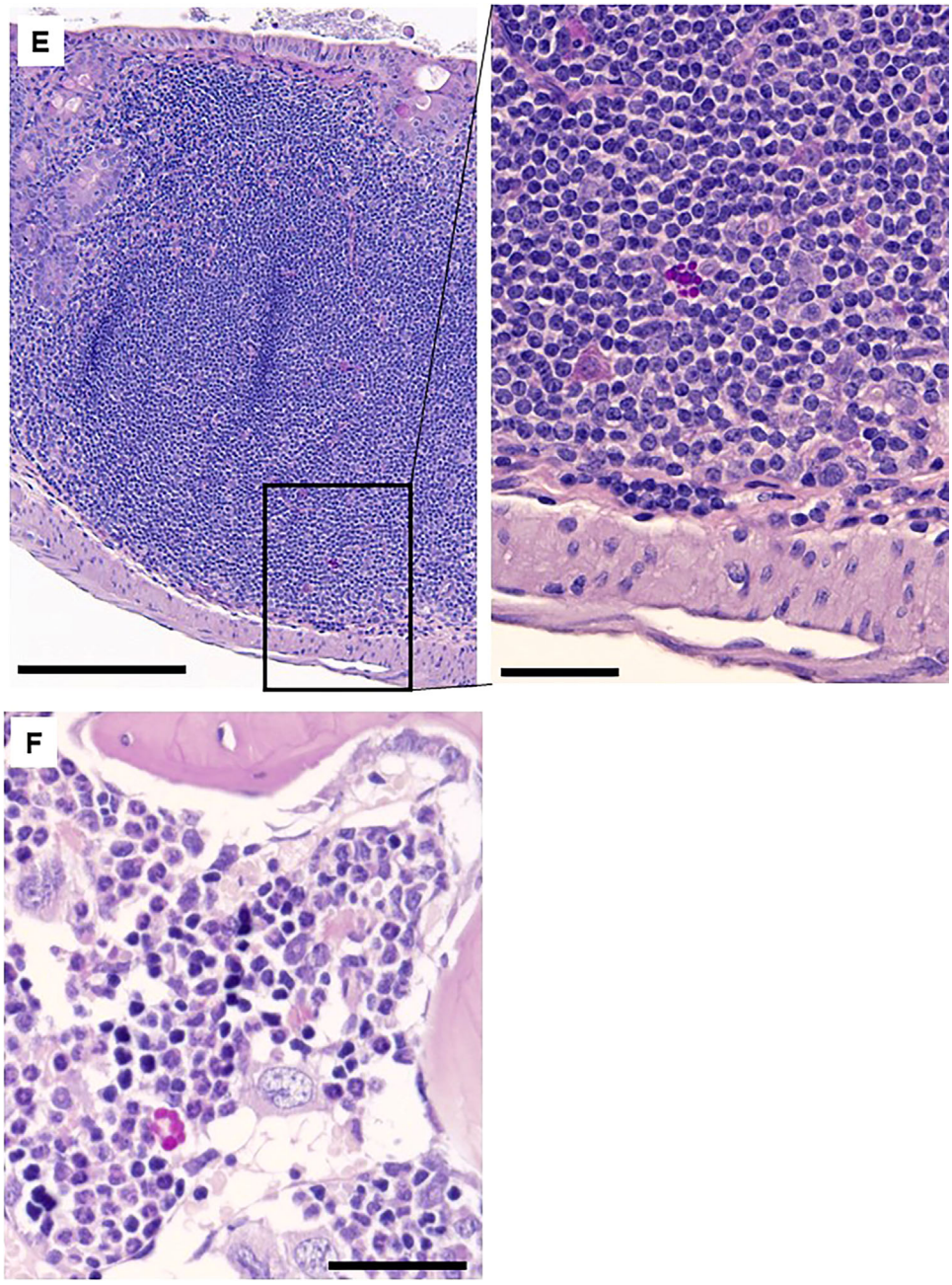


**Figure 2.** *Continued*

there from peripheral lymphoid tissues. Notably, these Mott cell tissue distributions were indistinguishable between *Fcmr* KO and their control mice, albeit the cells were much less frequent in the WT mice.

The frequency of Mott cells in peripheral lymphoid tissues was increased in all three strains of *Fcmr* KO mice as compared with the corresponding control mice (Fig. 3). In the 20-week-old female KO-NB strain, both generalized (*Cmv*/KO) and B cell-specific (*Cd19*/KO) FcμR deficiency, resulted in a significantly higher frequency of Mott cells in spleen than in WT controls ($p < 0.04$ and 0.01, respectively). The same was true for Mott cells in LNs of B cell-specific, *Fcmr* KO mice ($p < 0.02$). On the other hand, in the younger 15-week-old female KO-KHL strain, there was also an increasing trend of splenic Mott cell formation as B cell-specific *Fcmr* KO (*Cd19*/KO) > control *Cd19*-mediated *Cre*-expression ($Cd19^{Cre+/-}$) > another control floxed *Fcmr* ($Fcmr^{fl/fl}$), but such differences, particularly in *Cd19*/KO *versus* $Fcmr^{fl/fl}$, were not statistically significant ($p = 0.09$). In much older (60-wk) male KO-HO mice, there were markedly increased frequencies of Mott cells in spleen compared to WT controls ($p < 0.001$). Quantitative assessment of Mott cells in the BM cavity was unfortunately unsuccessful because of the irregular medullary shapes, which made it too difficult to assess the areas. Collectively, these findings indicated that: (i) Mott cells were present in peripheral

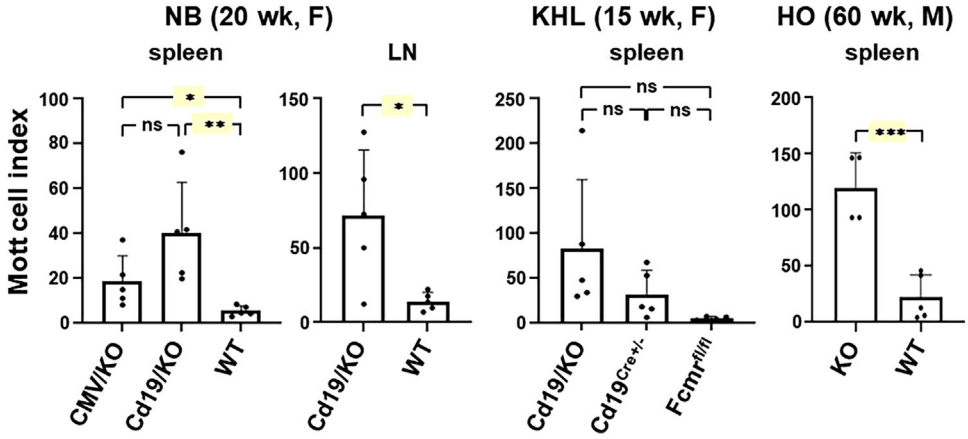


**Figure 3.** Incidence of Mott cells in spleen and lymph nodes from *Fcmr* KO and control mice. The indicated tissue blocks were obtained from generalized (CMV/KO) or B cell-specific (*Cd19*/KO) *Fcmr* KO mice of NO and their WT controls (left; 20 wk of age and female), B cell-specific (*Cd19*/KO) *Fcmr* KO mice of KHL and their corresponding controls ($Cd19^{Cre+/-}$ or $Fcmr^{fl/gl}$) (middle; 15 wk of age and female) and global *Fcmr* KO mice of HO and their WT controls (right; 60 wk of age and male). Tissue blocks were cut, deparaffinized, and stained with PAS reagent. Mott cell index is defined by 10 × the number of Mott cells per millimeter square. Each circle represents data from an individual mouse. Each group has five mice, except for *Fcmr* KO mice of HO ($n = 4$). Results are shown as mean ± 1 SD. Data comparison was performed by nonparametric analysis, Mann–Whitney for two groups and Kruskal-Wallis (with Dunn's multiple comparison test) for three groups. * $p < 0.05$, ** $p < 0.01$, *** $p < 0.001$ when compared with the corresponding controls.

lymphoid organs (i.e. spleen, LNs, Peyer's patches), in serosal fatty tissues and, to a lesser extent, in the BM; (ii) Mott cell formation was clearly increased in *Fcmr* KO mice irrespective of the targeted exons and deletion strategies; and (iii) such increases showed an age-dependent tendency.

## Generation of Mott cells in vitro and their immortalization by hybridoma technology

To determine the generation of Mott cells in vitro upon appropriate stimulations, splenic B cells from *Fcmr* KO (KO-HO) and WT mice were activated for 4 days at 37°C with three different stimuli: (i) LPS alone, (ii) LPS/dextran-anti-IgD/IL-4/IL-5 for preferential stimulation of B-1 B cells, and (iii) anti-CD40/dextran-anti-IgD/IL-4/IL-5 for preferential stimulation of B-2 B cells. Significantly fewer IgM-containing cells were seen in *Fcmr* KO B-cell cultures than in WT control B-cell cultures stimulated with LPS alone ($p < 0.05$) and a B-1 cocktail ($p < 0.05$), and a similar, but statistically insignificant, trend was also observed with a B-2 cocktail (Fig. 4A, left panel). By contrast, the frequencies of IgM-inclusion body-containing cells or Mott cells in mutant B-cell cultures were clearly increased compared to WT control B-cell cultures when stimulated with LPS alone ($p < 0.001$) or the B-1 stimulation cocktail ($p < 0.01$), but not with the B-2 stimulation cocktail (middle). The proportion of $\kappa^+$ cells among total $IgM^+$ cells was comparable in all the B-cell cultures (right). A similar increase in Mott cells was also observed with sorted B-1, but not B-2 B-cell cultures (not shown). These in vitro findings were, thus, consistent with the enhanced Mott cell formation in vivo *Fcmr* KO mice described above and with the previous findings that Mott cells were of B-1 B-cell origin [11, 35].

Next, to immortalize Mott cells, splenic B-1 B cells ($10^6$ cells) were enriched from *Fcmr* KO and WT control mice based on their co-expression of CD19 and CD5 (see Supporting Informationn Fig. S1) and activated ex vivo with LPS, before cell fusion. Sixteen and six B-1 hybridoma clones, corresponding to approximately 3.3 and 1.2% of the total plated wells, were thus, generated from *Fcmr* KO and WT mice, respectively. Even though Mott cells contain unique inclusion bodies in their cytoplasm, we could not distinguish Mott cell hybridomas from others based on examination by inverted phase-contrast microscopy. It is also noteworthy that Mott cells in single-cell suspension of lymphoid tissues could not be identified by flow cytometry based on their forward- and side-scatter characteristics. The identification of Mott cell hybridomas, thus, relied on PAS staining and staining of intracytoplasmic Ig in cell smears. Only one hybridoma clone (KO-03, μλ) derived from mutant mice exhibited Mott cell morphology characterized by the presence of inclusion bodies, strongly positive for PAS staining and for fluorochrome-labeled anti-μ and anti-λ antibody staining (Fig. 4B). Of the 16 mutant B-1 hybridomas, the Ig isotype distribution was 10 IgM (8 κ, 2 λ), 1 IgG3κ, 1 IgG2bκ, and 2 Ig-nonproducing, whereas among the six WT B-1 hybridomas, there were 4 IgM (3 κ, 1 λ), 1 IgG2bκ, and 1 Ig-nonproducing, as determined by both cytoplasmic Ig staining and enzyme-linked immunosorbent analysis of culture supernatants. For assessment of the self-reactivity of these B-1 B-cell hybridomas, Ag8.653 cell smears (fixed with 95% ethanol/5% glacial acetic acid) were used for indirect immunofluorescence analysis of culture supernatants. Four IgMκ-containing supernatants (three from mutant and one from WT mice) were found to react with the intracellular or plasma membrane components of Ag8.653. Consistent with the findings that most Mott hybridomas secrete small amounts of IgM [6], the KO-03 Mott hybridoma indeed secreted detectable amounts of IgMλ in culture supernatants (~0.6 μg/mL), but such

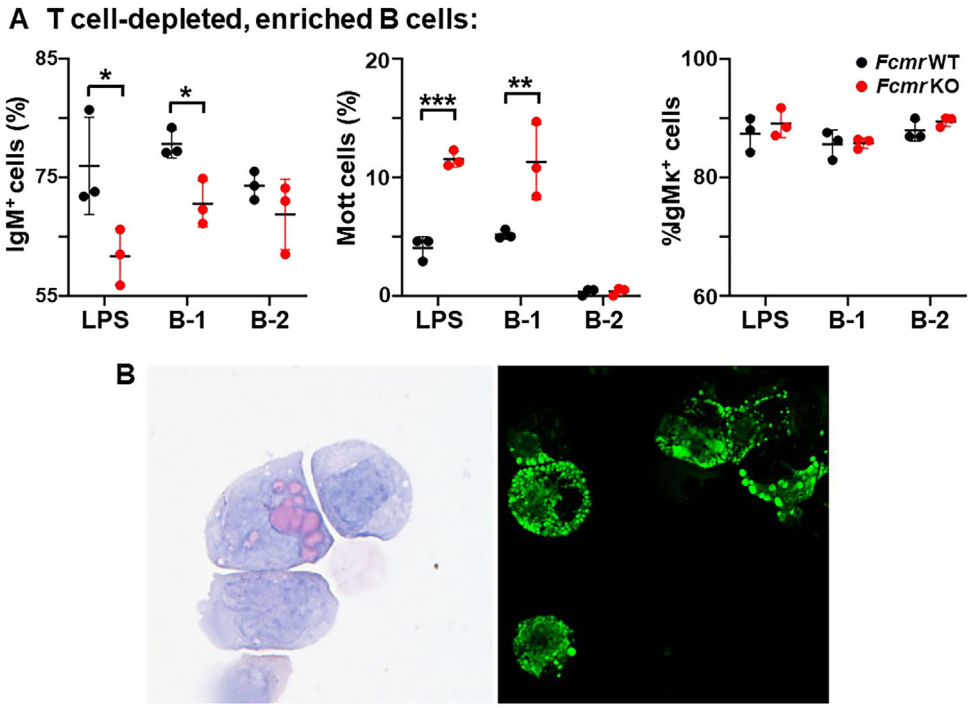


**Figure 4.** In-vitro generation of Mott cells and establishment of a Mott hybridoma clone from *Fcmr* KO mice. (A) Splenic B cells from *Fcmr* KO (red circles) and WT control (black circles) mice (13–14 wks, male) were cultured in triplicates for 4 days at 37°C in the presence of the indicated stimuli: LPS alone, B-1 stimulation cocktail (LPS/dextran-anti-IgD/IL-4/Il-5), or B-2 stimulation cocktail (anti-CD40/dextran-anti-IgD/IL-4/IL-5). The frequencies of IgM-producing plasmablasts or plasma cells (left), IgM inclusion body-containing cells or Mott cells (middle) and $\kappa^+$ cells among total $IgM^+$ cells (right) were assessed by cytoplasmic immunostaining of smears of cultured cells. Results are shown as mean ± 1 SD. Two-sided, independent Student's *t*-test was performed for statistical analysis. $^*p < 0.05$, $^{**}p < 0.01$, $^{***}p < 0.001$. (B) Mott hybridoma cells developed from LPS-stimulated splenic B-1 B cells of *Fcmr* KO mice were cytospun onto glass slides, air dried, fixed and washed, before staining with PAS reagent (left) and FITC-labeled goat anti-mouse μ antibodies (right). Note cytoplasmic inclusion bodies strongly stained with PAS (left) and FITC-anti-μ antibodies (right).

IgMλ did not react with Ag8.653 cellular components. These findings indicated the generation of a single Mott hybridoma by fusing splenic B-1 B cells in *Fcmr* KO mice with the Ag8.653 plasmacytoma line.

## Few mutations in Ig variable regions of the FcμR-deficient Mott cell hybridoma

To determine the nucleotide sequences of the Ig HC and LC variable regions (*Ighv* and *Iglv* ) of the Mott hybridoma, first-strand cDNA was generated from total RNA by RT-PCR using a set of primers for universal VH and Cμ1 and for Vλ2 and Cλ2. The nucleotide sequence analyses of the cloned PCR products revealed that the KO-03 clone utilized V1-55*01, D4-1*01, and J3*01 for its *Ighv* (Fig. 5A) and V2*02 and J2*01 for its *Iglv* (Fig. 5B). There were only three nucleotide mutations in the VH region (~99.0% identity of the germline V1-55*01) and six and five *N*-nucleotide additions at the VH/DH and of DH/JH junctions, respectively. The JH gene segment was identical to the germline J3*01. The variable region of Ig λ2 chain was 100% identical to the germline V2*02 and J2*01 sequences. The findings of few or no mutations in *Ighv* and *Iglv* and of *N*-nucleotide addition are consistent with the notion that Mott hybridomas are of adult B-1 B-cell origin with few mutations [35, 36].

## Reversal of the Mott cell phenotype by introduction of the FcμR

To determine if the expression of the FcμR can reverse the *Fcmr*-deficient Mott hybridoma to a normal plasma cell phenotype, the $IgM\lambda^+$ Mott hybridoma clone (KO-03) was transduced with a retroviral expression construct containing both mouse FcμR and GFP cDNAs (FcμR/GFP) or only GFP cDNA as an empty vector control. After enriching $GFP^+$ cells by fluorescence-activated cell sorting (FACS) and establishing individual stable transductants, the frequency of cells containing IgM inclusion bodies in their cytoplasm was assessed by immunofluorescence microscopic analysis at 3-week post-transduction. As shown in Fig. 6A, the frequency of cells containing IgM-inclusion bodies in the FcμR/GFP KO-03 transductants was significantly diminished as compared with that in the GFP only KO-03 transductants ($p < 0.01$) or in the original WT KO-03 Mott hybridoma ($p < 0.005$). No significant difference in the frequency of cells containing IgM-inclusion bodies was observed between the WT KO-03 hybridoma and

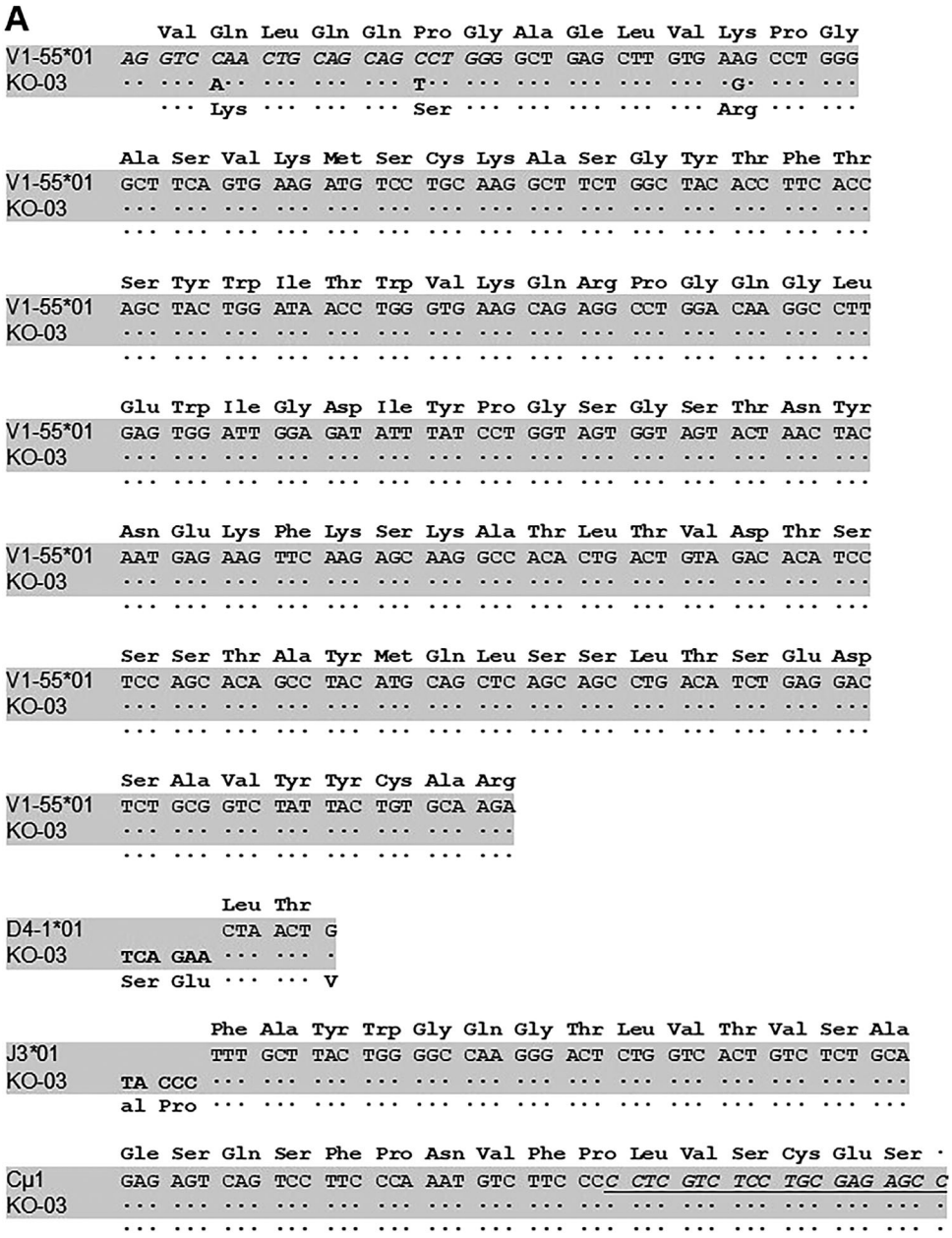


**Figure 5.** Nucleotide sequence of VH and Vλ2 of Mott hybridoma clone. The nucleotide sequence of VH (A) and Vλ2 (B) of IgMλ$^+$ Mott hybridoma clone (KO-03) and their translated amino acid sequences are indicated along with their corresponding germline gene segments. Sequence identity is indicated by dots (•) and the underlines indicate the sites corresponding to the primers described in the methods. The sequences have been deposited in GenBank under the accession numbers of OP426435 for the VH and OP426436 for the Vλ2 of Mott hybridoma KO-03 clone.

the GFP KO-03 transductants. Interestingly, the concentration of IgM secreted into the culture media was significantly higher in FcμR/GFP transductants than in GFP transductants and the Mott hybridoma, although the cell growth of these three cell lines was essentially similar (Fig. 6B). As expected, there was cell-surface expression of FcμR by FcμR/GFP transductants, but not by the control GFP transductants (Fig. 6C). Only the FcμR/GFP KO-03 transductants exhibited weak cell-surface IgM staining (Fig. 6D). Since these Ag8-derived transductants did not express CD79a (Igα)/CD79b (Igβ) (not shown), which are required for the cell-surface expression of membrane IgM, the observed surface IgM staining must result from the binding of pentameric IgM secreted by the FcμR/GFP KO-03 transductants to FcμR (cytophilic IgM). Given the fact that the assessment of IgM binding by mouse FcμR is usually difficult, this finding of cytophilic IgM was remarkable. Collectively, these findings strongly suggest a regulatory role of FcμR in the formation of Mott cells containing IgM-inclusion bodies.

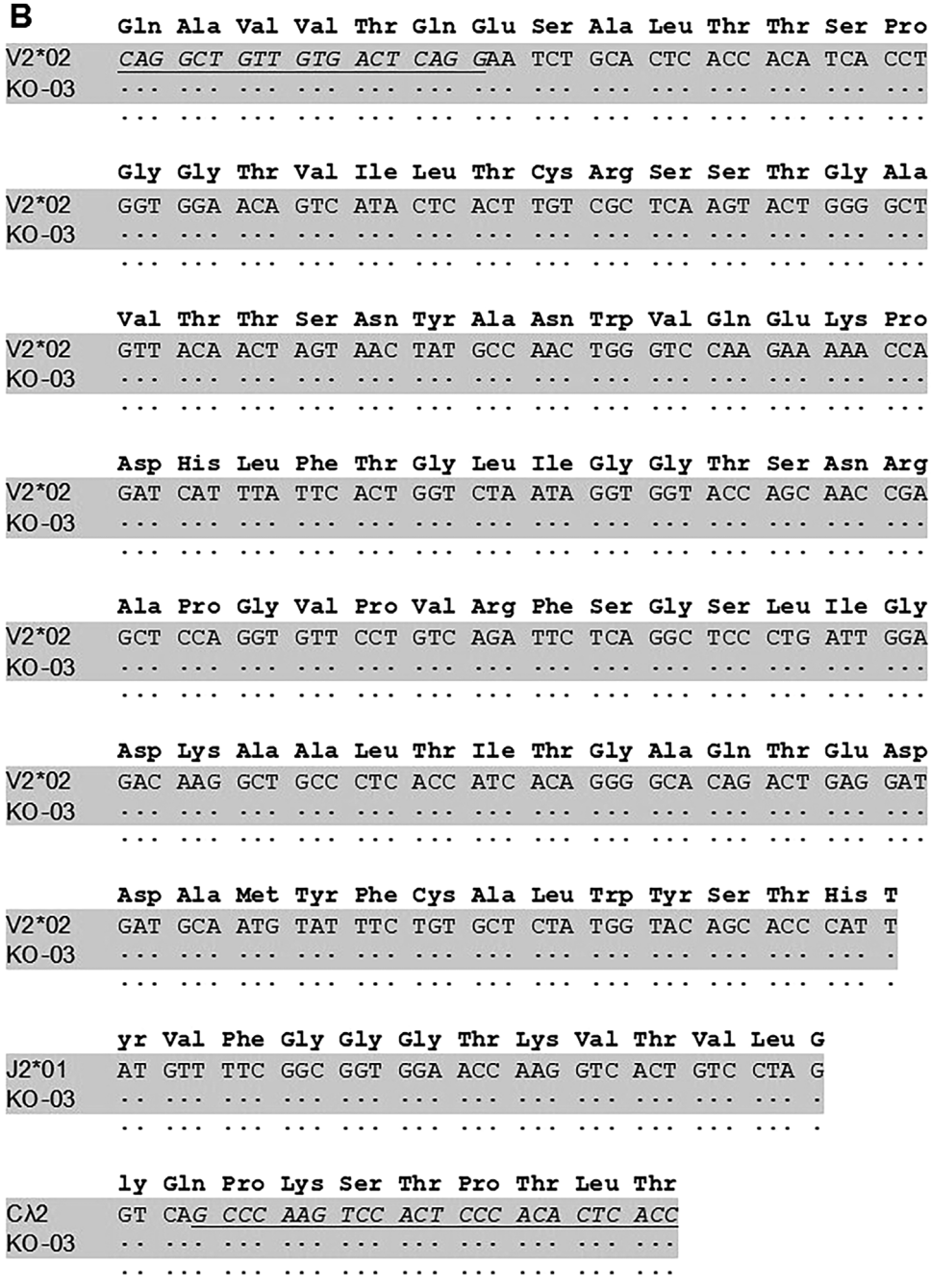


**Figure 5.** *Continued*

## Discussion

Conflicting results exist in terms of the phenotypes reported in five different FcμR-deficient mouse strains; one of the possible explanations for such discrepancies is differences in the gene targeting strategies [29]. The aim of the present study was to determine if the enhanced Mott cell formation observed in our mutant strain [33] is a generalized phenomenon associated with FcμR deficiency or a phenomenon unique to our strain. Comparative histological analysis was, thus, performed with three available different strains of *Fcmr* KO mice and their corresponding controls. The results showed a clear association of enhanced Mott cell formation with FcμR deficiency. Significantly high frequencies of Mott cells were generated from *Fcmr* KO mice than from WT controls when their splenic B cells or sorted B-1 B cells were stimulated in vitro with LPS alone or with the B-1 stimulation cocktail. By contrast, the B-2 stimulation cocktail did not generate Mott cells from splenic B cells or sorted B-2 B cells of either of the mouse groups, consistent with the previous findings of Mott cells of B-1 cell origin [11, 35]. A single IgMλ$^+$ Mott hybridoma clone was

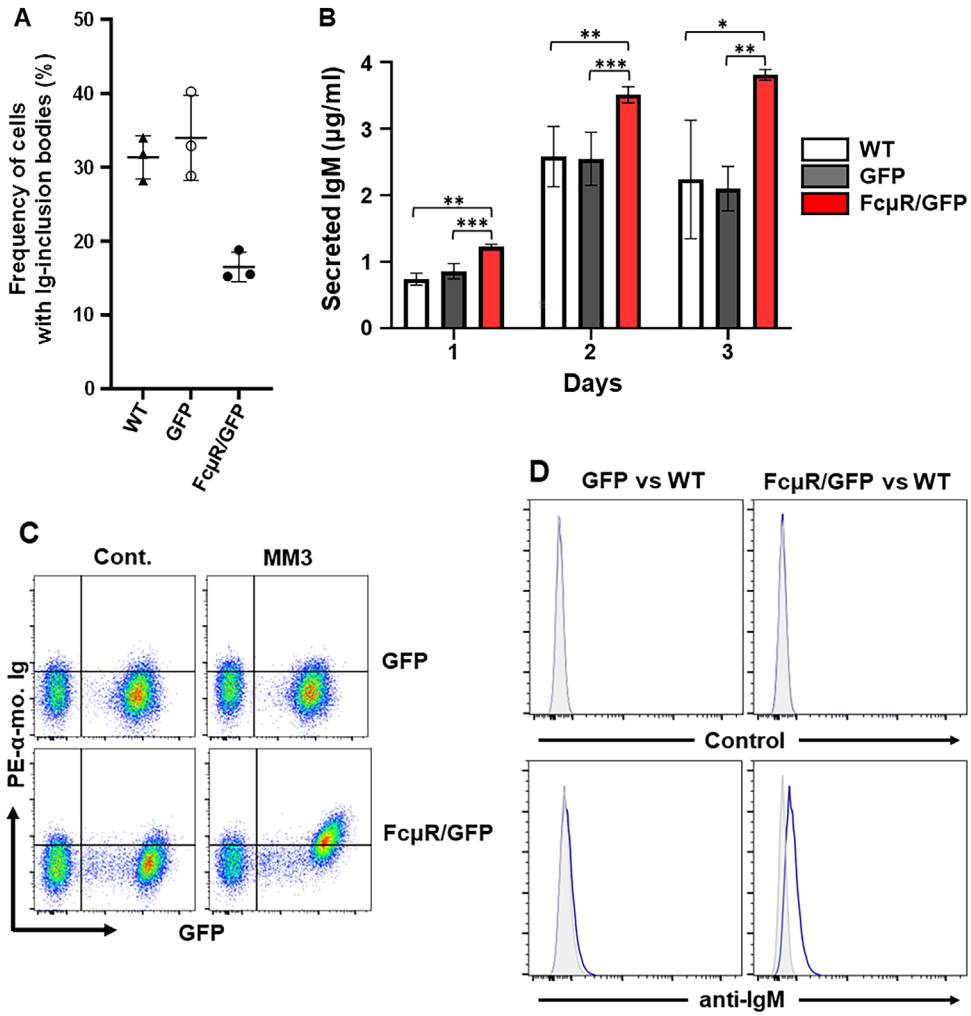


**Figure 6.** Reversal of the Mott phenotype by introduction of the FcμR. (A) Frequency (%) of cells carrying IgM-inclusion bodies in three cell lines: the original FcμR-deficient Mott hybridoma clone KO-03 (WT), KO-03 hybridoma transduced with empty vector containing GFP cDNA (GFP), and with vector containing both FcμR and GFP cDNAs (FcμR/GFP). Results are shown in mean ± 1 SD from three experiments. Note the significant reduction of cells containing Ig inclusion bodies in the FcμR/GFP transductants. $^{**}p < 0.01$. (B) ELISA for IgM secretion by the KO-03 Mott hybridoma and its GFP or FcμR/GFP transductants. KO-03 Mott hybridoma (white), GFP-transductants (black) and FcμR/GFP-transductants (red) were plated at $10^5$ cells/mL and IgM secreted into the media was assessed by ELISA during the 3-day culture. Results are shown as mean ± 1 SD from three different experiments. $^{*}p < 0.05$, $^{**}p < 0.01$, $^{***}p < 0.001$. (C) Flow cytometric analysis of FcμR expression. An equal number of cell mixture of the original KO-03 hybridoma and their FcμR/GFP (lower) or only GFP (upper) Mott hybridoma transductants was sequentially incubated with MM3 anti-FcμR (right) or isotype-matched (IgG1κ) control (left) mAb and then with PE-labeled goat anti-mouse Ig antibodies. (D) Passively acquired IgM on FcμR$^+$/GFP$^+$ Mott hybridoma transductant. PE-labeled rat anti-mouse IgM (lower panel) and PE-labeled isotype-matched control mAb (upper panel) were used to stain the cell surface of the KO-03 Mott hybridoma transduced with only GFP cDNA (left side) or FcμR/GFP cDNA (right side) and of the original KO-03 hybridoma (WT). The staining profiles of each transductant (clear) were overlayed to that of WT (gray).

generated from splenic B-1 B cells of our *Fcmr* KO mice and the nucleotide sequence analysis of the Ig variable regions revealed the nearly (VH) or complete (Vλ) identity with the corresponding germline gene segments (i.e. V1-55/D4-1/J3 and V2/J2). Introduction of FcμR into this Mott hybridoma resulted in a significant reduction of cells with IgM inclusion bodies and concomitantly in an increase in IgM secretion, suggesting the regulatory role of FcμR in the formation of Mott cells and Ig-inclusion or Russell bodies.

Mott cells-containing Ig inclusion bodies are rarely observed in normal lymphoid tissues but are found in various pathological conditions including neoplasms, inflammatory diseases, and autoimmune disorders [1, 2, 5, 6, 8, 14]. B-1, but not B-2, B cells were shown to generate Mott cells in vitro in the presence of LPS or IL-5 at a much higher frequency in autoimmune NZB and NZB/W F1 mice than in nonautoimmune NZW mice [11]. By using NZB/W F1 x NZW backcross mice, the locus contributing to Mott cell formation, called *Mott-1*, was mapped to a satellite marker locus between Mit48 and Mit70 on chromosome 4 of NZB mice [11]. Mott cells were also frequently observed in autoimmune "viable motheaten" mice that have a defect in protein tyrosine phosphatase SHP1/PTPN6 on chromosome 6 [5, 6]. B cell-specific deletion of *Ptpn6* promoted B-1 B-cell development, systemic autoimmunity, and increased Mott cells, like in

motheaten mice [36], suggesting a linkage of protein tyrosine phosphatase SHP1/PTNP6 deficiency with Mott cell formation. Intriguingly, T cells appeared to play a role in Mott cell formation, because Mott cells were rare in neonatally thymectomized motheaten mice and athymic nude NZB/W F1 mice [5, 11]. Thus, multiple genes or loci are apparently involved in the formation of Mott cells and Russell bodies.

There is a precedent in a transgenic mouse model that certain autoreactive B-cell hybridomas accumulate IgM in the Golgi due to the formation of immune complexes between IgM and glycosaminoglycan and release large spherical IgM complexes, termed spherons, of up to 2 μm in diameter [37]. As to the molecular basis for enhanced Mott cell formation in *Fcmr* KO mice, given their propensity to produce autoantibodies and the predominance of *cis* engagement of FcμR on the same cell surface, we proposed the following model [29]. A given B-cell expresses an IgM BCR with self-reactivity to an intracellular membrane component but may not interact with the corresponding antigen because of its low affinity. When the cell receives a certain signal to switch from the μm to μs exon usage (e.g. via a Toll-like receptor), along with the synthesis of J chain, during the translocation from ER to the Golgi, the resultant pentameric IgM is accumulated inside the vesicles, where it binds its cognate membrane antigen via the Fab regions and to FcμR via its Fc portion. This *cis* engagement of self-antigen/secreted pentameric IgM/FcμR within the vesicles prevents further development of such autoreactive B cells, thereby contributing to peripheral tolerance. Mott cells-containing Ig inclusion bodies are byproducts in the absence of FcμR. In the present study, we could not absolutely validate this model but did provide evidence that FcμR regulates the formation of Mott cells and Russell bodies.

Our initial concern was that the enhanced Mott cell formation we previously observed was a unique finding restricted to our mutant strain, because there was no description of this phenotype in other mutant strains. Of three *Fcmr* KO mice with different targeted exons (exon 2–4, only exon 4 vs. exon 4–7) and deletion strategies (generalized vs. B cell-specific), the incidence of Mott cells in peripheral lymphoid tissues was increased as compared to their control mice. The enhanced Mott cell formation is, thus, a general phenomenon associated with FcμR deficiency. Splenic B cells or B-1 B cells from *Fcmr* KO mice indeed generated more Mott cells than those from WT control mice upon activation in vitro with LPS or a B-1 stimulation cocktail, in agreement with the previous findings with autoimmune NZB strains of mice [11]. A single IgMλ$^+$ Mott hybridoma clone (KO-03) was developed from LPS-stimulated splenic B-1 B cells ($10^6$ cells) of *Fcmr* KO mice and carried a few mutations in *Ighv*, with several N additions at VH/DH and DH/JH junctions, and a germline *Iglv*. The paucity of somatic hypermutations in the Ig HC variable region (V1-55*01) is characteristic of B-1 B cells, consistent with the findings reported by others [35]. Despite the polyreactive nature of B-1 B cell-derived IgM, reactivity of IgMλ (KO-03) with the cytoplasm of Ag8.653 cells was undetectable by immunofluorescence analysis. Transduction of FcμR cDNA into this Mott hybridoma resulted in a clear reduction of the frequency of cells carrying IgM-inclusion bodies and acquiring secreted IgM through FcμR on the cell surface (cytophilic IgM). Since, we have experienced difficulty in clear-cut assessments of IgM ligand binding by mouse FcμR, unlike the human receptor, this finding of cytophilic IgM was noteworthy. The reversal of the Mott phenotype by introduction of FcμR strongly suggests the regulation of Mott cell and Russell body formation by the FcμR.

## Materials and methods

### Mice and ethics approval

*Fcmr* $^{-/-}$ (*Fcmr* KO) strain of C57BL/6 (B6) mouse origin, which was originally developed at the laboratory of Dr. Hiroshi Ohno [23] and designated KO-HO, was generated from its B6-backcrossed *Fcmr* $^{+/-}$ frozen embryos kindly provided by Dr. Takashi Kanaya (RIKEN Center for Integrative Medical Sciences, Yokohama, Japan), at the MPI for Infectious Biology in Berlin. The *Fcmr* genotype of resulting offspring was determined by genomic PCR of tail DNA using a diagnostic set of primers: diagnostic sets of primers: 5′-ctgtagggctgaggctgggctggtgacagg-3′ (forward), 5′-cgatggctaatatggcaatagtatgggatg-3′ (reverse), and 5′-cttctctcccatagtgtgggccatggtggc-3′ (reverse) corresponding to the 5′-flanking and 3′-flanking *Fcmr* exons 2 and 5, respectively as described [22]. All studies involving animals were conducted with approval of the Landesamt für Gesundheit und Soziales (Lageso) of the permission number of H 0126/16.

### Histopathological analysis

Formalin-fixed, paraffin-embedded tissue blocks (spleen, LNs, intestine, and postdecalcified long bones) were prepared from the *Fcmr* KO-HO and WT control mice. Similar tissue blocks of spleen and lymph nodes from two additional different strains of *Fcmr* KO B6 mouse as well as their corresponding controls were also provided for comparative analyses by each investigator: Dr. Nicole Baumgarth (NB) and Dr. Kyeong-Hee Lee (KHL). The age and sex of the analyzed mice were: KO-HO, 60-week-old and male [22, 23]; KO-NB, 20-week-old and female [31]; and KO-KHL, 15-week-old and female [32]. Tissue sections of approximately 4 μm in thickness were cut, deparaffinized, and stained with PAS (Sigma-Aldrich). Strongly PAS-positive plasma-like cells and spheres or Russell bodies were identified as Mott cells under Keyence Biorevo BZ-9000 microscopy (Keyence, Neu-Insenburg) and the frequency of Mott cells in a given area was estimated by computer.

### In-vitro generation of Mott cells

Erythrocyte-lysed splenocytes from *Fcmr* KO-HO and WT B6 mice (13-14 weeks, male) were incubated with a cocktail of biotinylated mAbs specific for CD3, CD4, and CD8 (Invitrogen) and then

with streptavidin-coated magnetic beads (Miltenyi), followed by magnetic cell sorting. The resultant erythrocyte- and T cell-depleted splenocytes were plated in triplicates at $2 \times 10^5$ cells/mL of RPMI 1640 containing 10% FCS, PC (100 U/mL)/SM (100 μg/mL), 50 μM 2-ME, fungizone (0.5 μg/mL), and gentamycin (5 μg/mL) (10% FCS complete medium) into 48-well plates (0.5 mL/well) and cultured at 37°C for 4 days in the presence of: (i) LPS (*E. coli*, SIGMA) (3 μg/mL), (ii) LPS (3 μg/mL)/dextran-coupled, rat anti-mouse IgD mAb (100 ng/mL; 11–26c clone, Fina Biosolutions)/IL-4 (6 ng/mL)/IL-5 (3 ng/mL; both BioLegend) for selective stimulation of B-1 B cells, or (iii) anti-CD40 mAb (10 μg/mL; FGK-45 clone)/dextran-anti-IgD mAb (100 ng/mL)/IL-4 (6 ng/mL)/IL-5 (3 ng/mL). In some experiment, splenic B cells from both groups of mice were incubated with allophycocyanin-labeled anti-CD19 (1D3; Invitrogen) and eFluor™ 450-labeled anti-CD5 mAbs (53-7.3; BioLegend) to sort $CD5^+/CD19^+$ B-1 B and $CD5^-/CD19^+$ B-2 B cells by FACS, prior to culture. After culturing and washing once with PBS/1% FCS, the cultured cells were cytocentrifuged onto glass slides, air dried, fixed in 95% ethanol/5% glacial acetic acid at −20°C for 20 min, and rehydrated in PBS, before staining with FITC-labeled goat anti-mouse μ and TRITC-labeled goat anti-mouse κ antibodies (both Southern Biotechnology Association) at 0.05 mg/mL for 20 min at room temperature. The stained cells were examined by confocal immunofluorescence microscopy.

## B-1 cell hybridomas

To immortalize Mott cells, similarly sorted $CD19^+/CD5^+$ B-1 B cells ($10^6$ cells) from three *Fcmr* KO-HO and six WT B6 mice (21–24 weeks, females) were resuspended in 1 mL of 20% FCS complete medium and stimulated with LPS at 50 μg/mL for 1 day. The resultant LPS-activated B-1 cells were fused with a threefold excess number of Ig nonproducing P3-X63-Ag8.653 cells [38] and were plated into 96-well flat-bottom plates at approximately $2 \times 10^3$ B-1 B cells/0.2 mL/well along with B6 peritoneal lavage cells as feeders. For detection of Mott cells, hybridoma cells were cytocentrifuged onto glass slides, and the resultant cell smears were stained for intracytoplasmic Igs with fluorochrome-labeled antibodies specific for each Ig isotype and for inclusion bodies with PAS staining as described [33].

## Sequence analyses of Ig HC and LC variable regions of Mott hybridomas

The nucleotide sequence of the Ig H and L chain V regions of the Mott hybridoma was determined by RT-PCR. In brief, 2 μg of the total RNA isolated from hybridoma cells by Trizol was converted to the first strand cDNA by using the SuperScript™ IV First-Strand Synthesis System (Invitrogen) with oligo$(dT)_{18}$ primers. The resultant first strand cDNA was used as a template DNA for amplification of the VH-Cμ1 and Vλ2-Cλ2 regions by using a set of primers [(i) universal coding VH (5'-aggtsmarctgcagsagtcwgg-3') and noncoding Cμ1 (5'-ggctctcgcaggagacgagg-3') and (ii) coding Vλ2 (5'-gccatttcccaggctgttgtgactcagg-3') and noncoding Cλ2 (5'-ggtgagwgtgggagtggacttgggc-3')] with Platinum SuperFi II DNA polymerase (Invitrogen). In IUPAC nucleotide code, m = a or c; r = a or g; s = g or c; w = a or t. The amplification was performed as follows: denaturation at 94°C for 1 min, 35 cycles of denaturation at 94°C for 20 s, annealing at 66°C (for VH-Cμ1) and 70°C (for Vλ2-Cλ2) for 20 s, and extension at 72°C for 80 s, and final extension at 72°C for 10 min. The amplified PCR products of VH-Cμ1 and Vλ2-Cλ2 with the expected size of approximately 400 and 360 bp, respectively, were gel purified and subcloned into pCR-Blunt II-Topo vector before nucleotide sequence analyses of the inserted PCR products in both strands by using Sp6 and T7 primers. The nucleotide sequence was analyzed by the IMGT/V-Quest [39] and IgBlast (NCBI) programs.

## Transduction

To determine the effect of mouse FcμR on the Ig-inclusion bodies in *Fcmr* KO B-1 B cell-derived Mott hybridoma, a bicistronic retroviral expression vector pRetroX-sGreen (Takara) containing mouse FcμR cDNA (FcμR/GFP) or no insert cDNA (GFP only) as a control was transfected into a PLAT-E packaging cell line, before transducing into Mott hybridoma cells as described [19]. After enriching $GFP^+$ cells by FACS, Mott hybridomas before and after transduction with mouse FcμR cDNA were examined for their expression of FcμR and IgM on their cell surface by flow cytometry.

## Flow cytometric analysis

For surface expression of FcμR and IgM, a mixture of original $GFP^-$ KO-03 Mott hybridoma cells and FcμR/GFP or GFP cDNA-transduced KO-03 Mott hybridoma cells were incubated with biotin-labeled mouse anti-mouse FcμR mAb (MM3 clone, γ1κ isotype) or rat anti-mouse μ mAb (RMM-1 clone, γ2aκ), washed, and then with PE-labeled streptavidin. Isotype-matched, irrelevant mAbs were included as controls. Stained cells were examined by BD FACSCanto II flow cytometry along with FACSDiva software (BD Bioscience), and flow cytometric data were analyzed with FlowJo software (Becton Dickinson).

**Acknowledgments:** We thank Takashi Kanaya and Hiroshi Ohno for providing $Fcmr^{+/-}$ frozen embryo; Anja Kühl for PAS staining; Ralf Uecker, Anja Hauser, and Vishnu Reddy for support of imaging analyses; Toralf Kaiser and Jenny Kirsch for flow cytometric and cell sorting; Andrew Lees for generous gift of dextran-coupled rat anti-IgD mAb; Hilmar Fünning for literature support; Hilmar Frank for information technology support; and Peter D. Burrows,

John F. Kearney, and Shozo Izui for critical reading and suggestions.
Open access funding enabled and organized by Projekt DEAL.

**Conflict of interest:** The author declares no conflict of interest.

**Author contributions:** KHL and NB provided the tissue blocks from their *Fcmr* KO and control mice. UK, PKJ, HK, and FM developed *Fcmr* KO mice from their frozen *Fcmr*$^{+/-}$ embryos. KAQ, KH, PMA, and HK conducted histological analysis (Fig. 2 and 3). HK, PKJ, KAQ, and PMA made B-1 B-cell hybridomas (Fig. 4 and Supporting Information Fig. S1), analyzed their nucleotide sequence (Fig. 5), and determined their phenotypes (Fig. 6). HK, FM, and AR wrote a paper and made Fig. 1. All authors contributed to the article and approved the submitted version.

**Data availability statement:** The data that support the findings of this study are available on request from the corresponding author.

**Peer review:** The peer review history for this article is available at https://publons.com/publon/10.1002/eji.202250315

## References

1 **Bain, B. J.**, Russell bodies and Mott cells. *Am. J. Hematol.* 2009. **84**: 516.

2 **Bangle R., Jr**, A morphologic and histochemical study of cytoplasmic Russell bodies in cancer cells. *Am. J. Pathol.* 1963. **43**: 437–448.

3 **Weiss, S., Burrows, P. D., Meyer, J. and Wabl, M. R.**, A Mott cell hybridoma. *Eur. J. Immunol.* 1984. **14**: 744–748.

4 **Alanen, A., Pira, U., Lassila, O., Roth, J. and RM, F.**, Mott cells are plasma cells defective in immunoglobulin secretion. *Eur. J. Immunol.* 1985. **15**: 235–242.

5 **Shultz, L. D., Coman, D. R., Lyons, B. L., Sidman, C. L. and Taylor, S.**, Development of plasmacytoid cells with Russell bodies in autoimmune "viable motheaten" mice. *Am. J. Pathol.* 1987. **127**: 38–50.

6 **Schweitzer, P. A., Taylor, S. E. and Shultz, L. D.**, Synthesis of abnormal immunoglobulins by hybridomas from autoimmune "viable motheaten" mutant mice. *J. Cell Biol.* 1991. **114**: 35–43.

7 **Valetti, C., Grossi, C. E., Milstein, C. and Sitia, R.**, Russell bodies: a general response of secretory cells to synthesis of a mutant immunoglobulin which can neither exit from, nor be degraded in, the endoplasmic reticulum. *J. Cell Biol.* 1991. **115**: 983–994.

8 **Maldonado, J. E., Brown A. L., Jr., Bayrd, E. D. and Pease, G. L.**, Cytoplasmic and intranuclear electron-dense bodies in the myeloma cell. *Arch. Pathol.* 1966. **81**: 484–500.

9 **Posnett, D. N., Mouradian, J., Mangraviti, D. J. and DJ, W.**, Mott cells in a patient with a lymphoproliferative disorder Differentiation of a clone of B lymphocytes into Mott cells. *Am. J. Med.* 1984. **77**: 125–130.

10 **van Greune, C. H., Slazus, W. and DJ, R.**, Circulating Russell-body-containing lymphoid cells in an immunocytoma patient. *Acta Haematol.* 1994. **91**: 108–110.

11 **Jiang, Y., Hirose, S., Hamano, Y., Kodera, S., Tsurui, H., Abe, M. Terashima, K. et al.**, Mapping of a gene for the increased susceptibility of B1 cells to Mott cell formation in murine autoimmune disease. *J. Immunol.* 1997. **158**: 992–997.

12 **Martin-Noya, A., Rios-Herranz, E. and Rafel-Ribas, E.**, Multiple myeloma with numerous intranuclear Russell bodies. *Haematologica* 1999. **84**: 179–180.

13 **Krishnan, B. and Thiagarajan, P.**, Images in hematology. Myeloma with Russell bodies. *Am. J. Hematol.* 2005. **78**: 79.

14 **Pizzolitto, S., Camilot, D., DeMaglio, G. and Falconieri, G.**, Russell body gastritis: expanding the spectrum of *Helicobacter pylori*-related diseases? *Pathol. Res. Pract.* 2007. **203**: 457–460.

15 **Kopito, R. R. and Sitia, R.**, Aggresomes and Russell bodies. Symptoms of cellular indigestion? *EMBO Rep.* 2000. **1**: 225–231.

16 **Decourt, C., Galea, H. R., Sirac, C. and Cogne, M.**, Immunologic basis for the rare occurrence of true nonsecretory plasma cell dyscrasias. *J. Leukoc. Biol.* 2004. **76**: 528–536.

17 **Mattioli, L., Anelli, T., Fagioli, C., Tacchetti, C., Sitia, R. and Valetti, C.**, ER storage diseases: a role for ERGIC-53 in controlling the formation and shape of Russell bodies. *J. Cell Sci.* 2006. **119**(Pt 12): 2532–2541.

18 **Corcos, D., Osborn, M. J., Matheson, L. S., Santos, F., Zou, X., Smith, J. A., Morgan, G. et al.**, Immunoglobulin aggregation leading to Russell body formation is prevented by the antibody light chain. *Blood* 2010. **115**: 282–288.

19 **Kubagawa, H., Oka, S., Kubagawa, Y., Torii, I., Takayama, E., Kang, D. W., Gartland, GL. et al.**, Identity of the elusive IgM Fc receptor (FcμR) in humans. *J. Exp. Med.* 2009. **206**: 2779–2793.

20 **Murakami, Y., Narayanan, S., Su, S., Childs, R., Krzewski, K., Borrego, F., Weck, J. et al.**, Toso, a functional IgM receptor, is regulated by IL-2 in T and NK cells. *J. Immunol.* 2012. **189**: 587–597.

21 **Shima, H., Takatsu, H., Fukuda, S., Ohmae, M., Hase, K., Kubagawa, H., Wang, JY. et al.**, Identification of TOSO/FAIM3 as an Fc receptor for IgM. *Int. Immunol.* 2010. **22**: 149–156.

22 **Honjo, K., Kubagawa, Y., Jones, D. M., Dizon, B., Zhu, Z., Ohno, H., Izui, S. et al.**, Altered Ig levels and antibody responses in mice deficient for the Fc receptor for IgM (FcμR). *Proc. Natl. Acad. Sci. USA.* 2012. **109**: 15882–15887.

23 **Ouchida, R., Mori, H., Hase, K., Takatsu, H., Kurosaki, T., Tokuhisa, T., Ohno, H. et al.**, Critical role of the IgM Fc receptor in IgM homeostasis, B-cell survival, and humoral immune responses. *Proc. Natl. Acad. Sci. USA.* 2012. **109**: E2699–E2706.

24 **Kubagawa, H., Skopnik, C. M., Zimmermann, J., Durek, P., Chang, H. D., Yoo, E., Bertoli, L. F. et al.**, Authentic IgM Fc receptor (FcμR). *Curr. Top. Microbiol. Immunol.* 2017. **408**: 25–45.

25 **Honjo, K., Kubagawa, Y., Kearney, J. F. and Kubagawa, H.**, Unique ligand-binding property of the human IgM Fc receptor. *J. Immunol.* 2015. **194**: 1975–1982.

26 **Kubagawa, H., Kubagawa, Y., Jones, D., Nasti, T. H., Walter, M. R. and Honjo, K.**, The old but new IgM Fc receptor (FcμR). *Curr. Top. Microbiol. Immunol.* 2014. **382**: 3–28.

27 **Skopnik, C. M., Al-Qaisi, K., Calvert, R. A., Enghard, P., Radbruch, A., Sutton, B. J. and Kubagawa, H.**, Identification of amino acid residues in human IgM Fc receptor (FcmicroR) critical for IgM binding. *Front. Immunol.* 2021. **11**: 618327.

28 **Kubagawa, H., Skopnik, C. M., Al-Qaisi, K., Calvert, R. A., Honjo, K., Kubagawa, Y., Teuber, R. et al.**, Differences between human and mouse IgM Fc receptor (FcmicroR). *Int. J. Mol. Sci.* 2021. **22**: 7024.

29 **Kubagawa, H., Honjo, K., Ohkura, N., Sakaguchi, S., Radbruch, A., Melchers, F. and Jani, P. K.**, Functional roles of the IgM Fc receptor in the immune system. *Front. Immunol.* 2019. **10**: 945.

30 **Choi, S. C., Wang, H., Tian, L., Murakami, Y., Shin, D. M., Borrego, F., Morse, H. C. et al.**, Mouse IgM Fc receptor, FCMR, promotes B cell development

and modulates antigen-driven immune responses. *J. Immunol.* 2013. **190**: 987–996.

31 **Nguyen, T. T., Klasener, K., Zurn, C., Castillo, P. A., Brust-Mascher, I., Imai, D. M., Bevins, C. L. et al.**, The IgM receptor FcμR limits tonic BCR signaling by regulating expression of the IgM BCR. *Nat. Immunol.* 2017. **18**: 321–333.

32 **Yu, J., Duong, V. H. H., Westphal, K., Westphal, A., Suwandi, A., Grassl, G. A, Brand, K. et al.**, Surface receptor Toso controls B cell-mediated regulation of T cell immunity. *J. Clin. Invest.* 2018. **128**: 1820–1836.

33 **Honjo, H., Kubagawa, Y., Suzuki, Y., Takagi, M., Ohno, H., Bucy, R. P., Izui, S. et al.**, Enhanced autoantibody and Mott cell formation in FcμR-decient autoimmune mice. *Int. Immunol.* 2014. **26**: 659–672.

34 **Alanen, A., Pira, U., Colman, A. and RM, F.**, Mott cells: A model to study immunoglobulin secretion. *Eur. J. Immunol.* 1987. **17**: 1573–1577.

35 **Tarlinton, D., Forster, I. and Rajewsky, K.**, An explanation for the defect in secretion of IgM Mott cells and their predominant occurrence in the Ly-1 B cell compartment. *Eur. J. Immunol.* 1992. **22**: 531–539.

36 **Pao, L. I., Lam, K. P., Henderson, J. M., Kutok, J. L., Alimzhanov, M., Nitschke, L., Thomas, M. L. et al.**, B cell-specific deletion of protein-tyrosine phosphatase Shp1 promotes B-1a cell development and causes systemic autoimmunity. *Immunity* 2007. **27**: 35–48.

37 **Khan, S. N., Cox, J. V., Nishimoto, S. K., Chen, C., Fritzler, M. J., Hendershot, L. M., Weigert, M. et al.**, Intra-Golgi formation of IgM-glycosaminoglycan complexes promotes Ig deposition. *J. Immunol.* 2011. **187**: 3198–3207.

38 **Kearney, J. F., Radbruch, A., Liesegang, B. and Rajewsky, K.**, A new mouse myeloma cell line that has lost immunoglobulin expression but permits the construction of antibody-secreting hybrid cell lines. *J. Immunol.* 1979. **123**: 1548–1550.

39 **Brochet, X., Lefranc, M. P. and Giudicelli, V.**, IMGT/V-QUEST: The highly customized and integrated system for IG and TR standardized V-J and V-D-J sequence analysis. *Nucleic Acids Res.* 2008. **36**: W503–W508.

*Abbreviations:* **FcμR**: Fc receptor for IgM · **HC**: heavy chain · **HO**: Hiroshi Ohno · **KHL**: Kyeong-Hee Lee · **LCs**: light chains · **NB**: Nicole Baumgarth · **RT-PCR**: reverse transcription-polymerase chain reaction

*Full correspondence:* Prof. Hiromi Kubagawa, Deutsches Rheuma-Forschungszentrum (DRFZ), Berlin, Germany.
e-mail: hiromi.kubagawa@drfz.de

Received: 6/12/2022
Revised: 31/3/2023
Accepted: 25/4/2023
Accepted article online: 26/4/2023